Meso Scale Modeling with a Reynolds Averaged Navier–Stokes Solver

Assessment of wind resources along the Norwegian coast

by

Arne R. Gravdahl
gravdahl@vector.no

VECTOR AS, Nedre Vargvei 32, N-3124 Tønsberg, Norway
http://vector.no

31th IEA Experts Meeting
State of the Art on Wind Resource Estimation
Risø Denmark, October 1998

Contents

1 Introduction

Although the wind climate in Norway seems favourable, the exploitation of wind energy has so far been very modest. However, recently the general interest for wind energy has increased. Wind measurements are currently carried out at about 30-40 locations. The Norwegian Water Resources and Energy Administration (NVE) receives an increasing number of applications for erecting wind turbines. On this background NVE has decided to launch a project on meso scale wind modeling.

The meso scale modeling will cover the Norwegian coast line from the southern tip at Lindesnes up to the Russian border in the north. About 100-150 models with an extension of approximately $30 \times 30 \times 3$ km will cover the coast. A windrose will be associated to each model, with annual and seasonal mean wind speeds. The windroses will be established based on long term statistical weather data from 30 meteorological stations situated along the coast. Micro models will be established for some of the meteorological stations in order to correct for terrain induced speed–up effects.

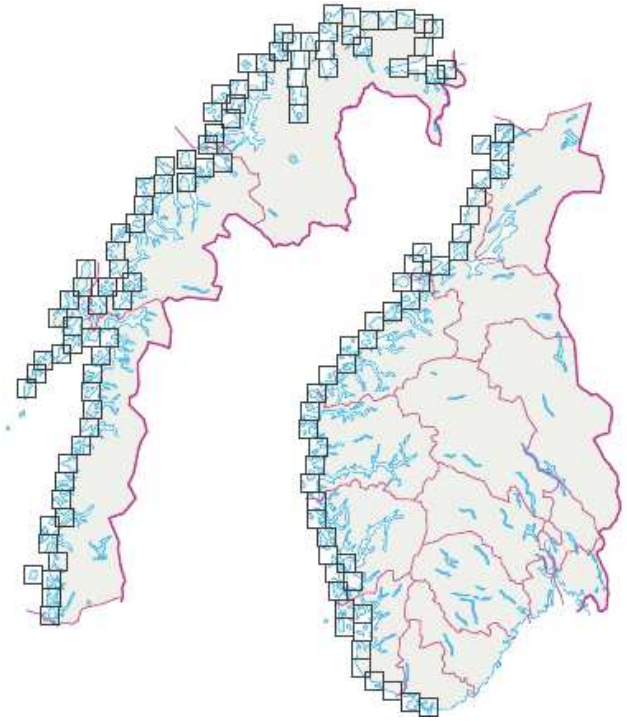

Figure 1: Meso scale models along the Norwegian coast, preliminary outline

The meso scale modeling will be undertaken in 1999. At present, verifications in several terrains with various geometrical complexity have been carried out. Description of the simulation tool and results from the verifications will be presented herein.

2 WIND–SIM a Reynolds averaged Navier–Stokes solver

WIND–SIM is a simulator for prediction of local wind fields and dispersion of air pollution. It is based on the general purpose CFD code PHOENICS. PHOENICS is an

open code allowing users to add their own subroutines, a useful feature when simulating the atmospheric boundary layer (ABL), [Näslund et al. (1992)], [Grundberg (1994)], [Alm and Nygaard (1995)] and [Baklanov et al. (1997)]

2.1 Turbulence modelling

In connection with wind energy the wind field on meso and micro scale can be described by the steady state incompressible Reynolds averaged Navier–Stokes equations, given in standard notation.

$$\frac{\partial U_i}{\partial x_i} = 0 \tag{1}$$

$$U_j \frac{\partial U_i}{\partial x_j} = -\frac{1}{\rho}\frac{\partial P}{\partial x_i} + \frac{\partial}{\partial x_j}\left(\nu\left(\frac{\partial U_i}{\partial x_j} + \frac{\partial U_j}{\partial x_i}\right) - (\overline{u_i u_j})\right) \tag{2}$$

In order to close the set, the turbulent Reynolds stresses are related to the mean velocity variables through the turbulent viscosity ν_T.

$$\overline{u_i u_j} = -\nu_T\left(\frac{\partial U_i}{\partial x_j} + \frac{\partial U_j}{\partial x_i}\right) + \frac{2}{3}\delta_{ij}k \tag{3}$$

Further the $k-\varepsilon$ model is used to relate the turbulent viscosity to k and ε, the turbulent kinetic energy and its dissipation rate.

$$\nu_T = c_\mu \frac{k^2}{\varepsilon} \tag{4}$$

$$\frac{\partial}{\partial x_i}(U_i k) = \frac{\partial}{\partial x_i}\left(\frac{\nu_T}{\sigma_k}\frac{\partial k}{\partial x_i}\right) + P_k - \varepsilon \tag{5}$$

$$\frac{\partial}{\partial x_i}(U_i \varepsilon) = \frac{\partial}{\partial x_i}\left(\frac{\nu_T}{\sigma_\varepsilon}\frac{\partial \varepsilon}{\partial x_i}\right) + c_{\varepsilon 1}\frac{\varepsilon}{k}P_k - c_{\varepsilon 2}\frac{\varepsilon^2}{k} \tag{6}$$

Where the turbulent production term P_k is:

$$P_k = \nu_T\left(\frac{\partial U_i}{\partial x_j} + \frac{\partial U_j}{\partial x_i}\right)\frac{\partial U_i}{\partial x_j} \tag{7}$$

The model constants in the so called standard $k-\varepsilon$ model have been found to take the values given in Table 1.

c_μ	σ_k	σ_ε	$c_{\varepsilon 1}$	$c_{\varepsilon 2}$
0.09	1.0	1.3	1.44	1.92

Table 1: Values of the model constants in the standard $k-\varepsilon$ model

The model constants in the standard $k-\varepsilon$ model have been tuned to fit some basic flow problems; shear layer in local equilibrium; decaying grid turbulence and a boundary layer

where the logarithmic velocity profile prevails. The model is not very general, typically the model constants have been adjusted in order to mimic other flow regimes.

Considering a neutral ABL, the standard $k-\varepsilon$ model is unable to reproduce the right level of turbulence in the weak shear layer away from the ground. In this region the turbulent viscosity is overpredicted, [Detering and Etling (1985)].

The standard model constants have been modified in an attempt to improve the situation. The value of $c_{\varepsilon 2}$, determined from experiments with decaying grid turbulence, remains unchanged. The diffusion constant σ_k, close to unity following Reynolds analogy, also remains unchanged. Whereas the constant c_μ, determined from a shear layer in local equilibrium where c_μ is found to be equal to $(\overline{u_1 u_2}/k)^2$, has been reduced in accordance with measurements in the ABL [Panofsky et al. (1977)]. Finally, the constants $c_{\varepsilon 1}$ and σ_ε can been adjusted, guided by the relation from a boundary layer where the logarithmic law is valid:

$$c_{\varepsilon 1} = c_{\varepsilon 2} - \frac{\kappa^2}{\sqrt{c_\mu}\sigma_\varepsilon} \tag{8}$$

In this work the modified model constants given in table 2 have been tested.

c_μ	σ_k	σ_ε	$c_{\varepsilon 1}$	$c_{\varepsilon 2}$
0.0324	1.0	1.85	1.44	1.92

Table 2: Values of the model constants in the modified $k-\varepsilon$ model

2.2 Boundary conditions

Wall functions are applied along the ground. At the first node at distance d above the ground particular relations are imposed. The velocity profile is logarithmic with the inclusion of roughness. The turbulence is assumed to be in local equilibrium yielding:

$$k = \frac{U_\tau^2}{\sqrt{c_\mu}} \tag{9}$$

$$\varepsilon = \frac{U_\tau^3}{\kappa d} \tag{10}$$

Here the friction velocity is defined as $U_\tau = \sqrt{\tau_w/\rho}$, the von Karman constant κ is set equal to 0.4. Profiles for velocity, k and ε are imposed at the inlet. The profiles are developed in a numerical sub-model. Due to the anomaly of the standard $k-\varepsilon$ model in weak shear layers, as discussed above, analytical profiles for k and ε have also been tested. The analytical profiles are taken from [Huser et al. (1997)].

$$k = \frac{U_\tau^2}{\sqrt{c_\mu}}\left(1 - \frac{z}{h}\right)^2 \tag{11}$$

$$\varepsilon = \frac{U_\tau^3}{\kappa}\left(\frac{1}{z} + \frac{4}{L}\right) \tag{12}$$

Here h is the boundary layer depth, $h = 0.4\sqrt{U_\tau L/f}$, where f is the Coriolis parameter and L is the Obukov length taken as 10 000 meter for a neutral atmosphere.

3 Verification

This verification starts with a simple flat terrain and moves on towards more complex geometries. In general, numerical simulations can be contaminated with grid dependencies. Grid independent solutions is achieved by refinement of the grid, which in practical situations is very demanding with respect to computational costs. Therefore, it is important to gain insight into the errors made when modelling with grids too coarse to reflect the underlying topography.

3.1 Flat uniform terrain

Simulations over flat terrain have been carried out with varying roughness heights z_0. The boundary layer height has been set to 500 m, and the velocity profile is assumed to follow the logarithmic law.

$$\frac{U}{U_\tau} = \frac{1}{\kappa} ln \frac{z}{z_0} \tag{13}$$

The grid distributions are given in figure 2. The grid is refined towards the ground, the grading factor defines the ratio between the cell size at the lower and upper boundary. Resulting speeds at 50 above the ground are given in the same figure, as expected grid refinement improves the results. The standard $k-\varepsilon$ model was used, the modified model gave slightly larger discrepancies versus the logarithmic law.

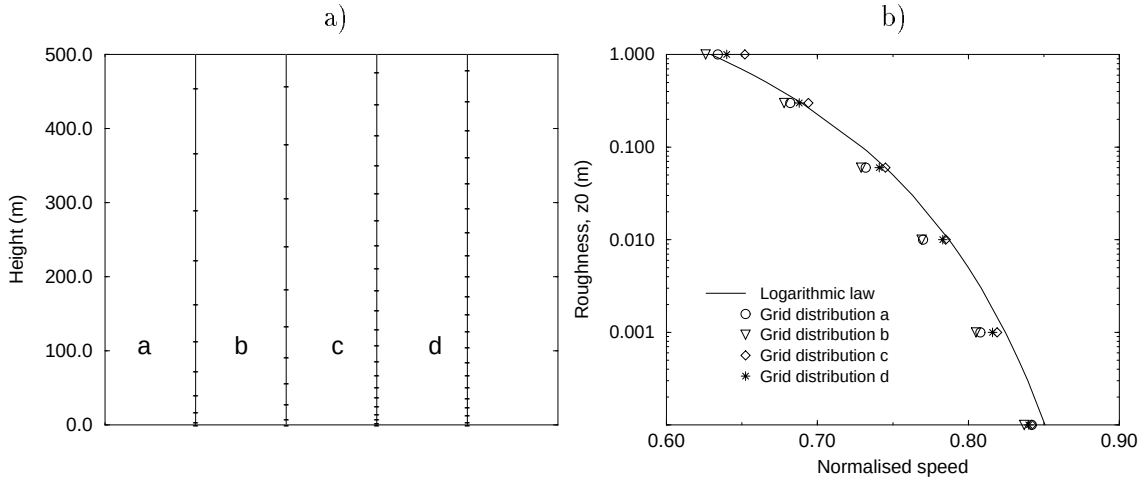

Figure 2: Flat uniform terrain
a) Grid distributions
b) Normalised speed at 50 meter, against roughness height

3.2 2D Hill

Speed–ups for simplified geometries are summarised in [Lemelin et al. (1988)]. The 2D hill given in figure 3 is reported to have a maximum speed–up of 0.65. The 2D hill has a characteristic slope of 0.28 (hill height/hill length) and a normalised roughness of 2.8 10^3

(hill length/roughness height). Speed–ups found in this work is depicted in figure 4. The grid dependency is not particularly significant, more remarkable is the variation due to the chosen turbulence model. The standard $k-\varepsilon$ model gives speed–ups in the order of 0.65, while with the modified turbulence model the speed–up is only 0.52. In figure 4 the streamwise velocity component along the ground is also depicted. Separation is observed with the standard $k-\varepsilon$ model, but not with the modified version.

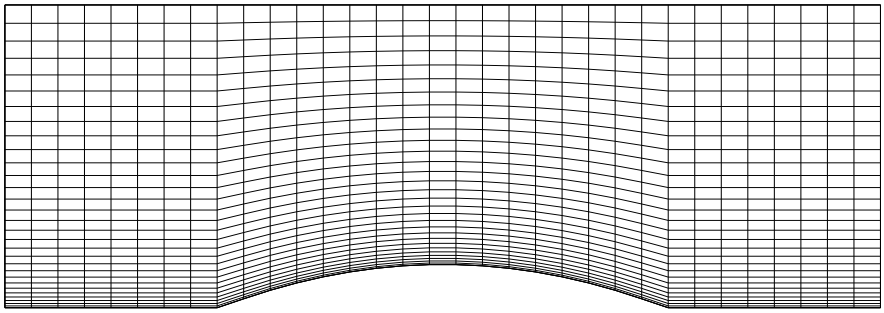

Figure 3: Grid distribution for 2D hill

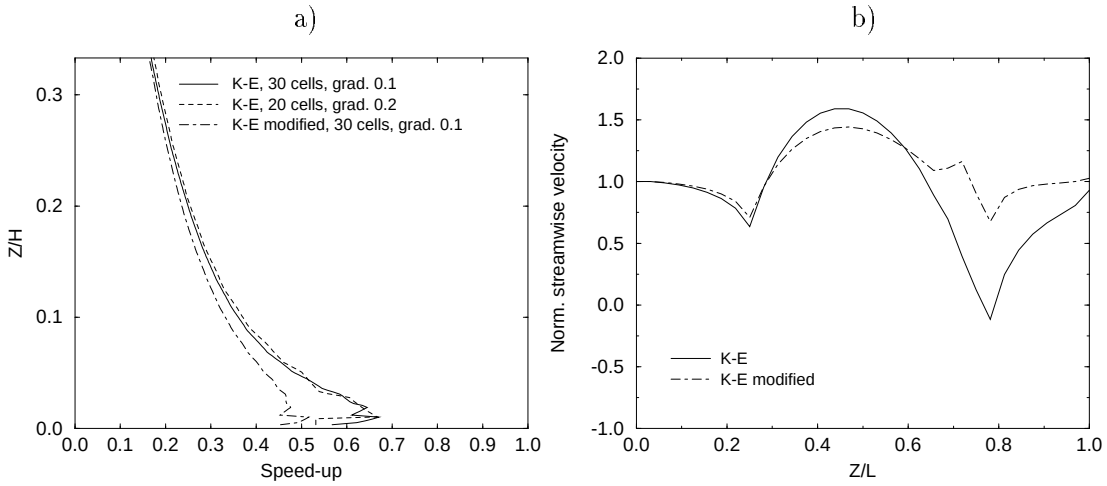

Figure 4: 2D hill
a) Speed-up at hill top
b) Normalised speed in streamwise direction, just above the ground

3.3 Askervein Hill

Field experiments were carried out at Askervein Hill in 1982 – 1983, as summarised in [Taylor and Teunissen (1987)]. The hill resembles an ellipsoid with major and minor axis

of approximately 2 km and 1 km respectively. Maximum hill height is 116 m. An area with approximate extensions $3000 \times 3000 \times 1100$ meter is discretised with $40 \times 50 \times 30$ cells. Grid refinement is used in streamwise direction (flow direction from left to right) giving the finest grid near the hill top in the order of 40 meter, and in vertical direction giving the first cell height at approximately 3 meter. The topography is given in figure 5, which also presents the two lines A and AA where field experiments are available. Normalised speed–ups are given in figure 6. As seen for the simple 2D hill, the modified $k-\varepsilon$ model underpredicts the speed–up. As for the 2D hill the modified $k-\varepsilon$ model does not separate on the lee side. Details of the 3D separation zone is given in figure 7, giving the velocity field at a height of 10, which is just above the region with reversed flow.

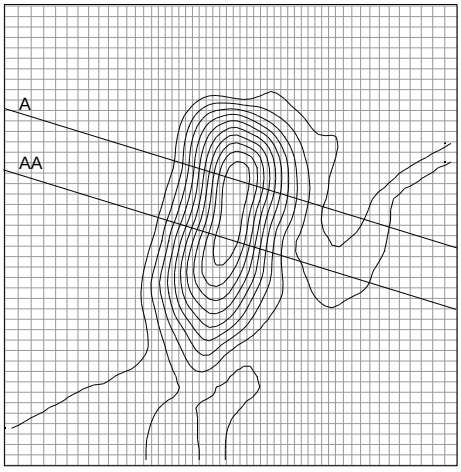

Figure 5: Grid distribution and topography for Askervein Hill, contour interval is 10 meter

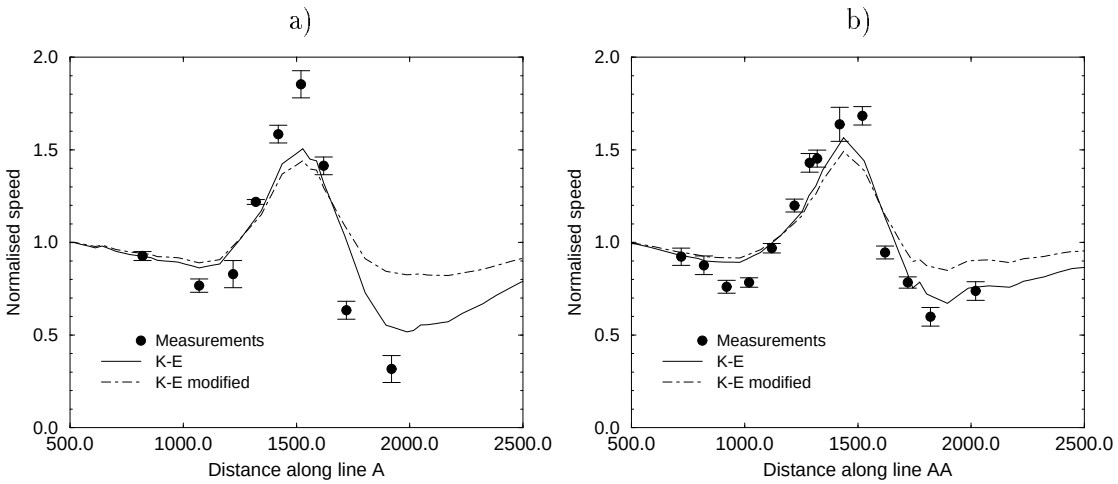

Figure 6: Normalised speed over Askervein Hill
a) Along line A, 10 meters above ground
b) Along line AA, 10 meters above ground

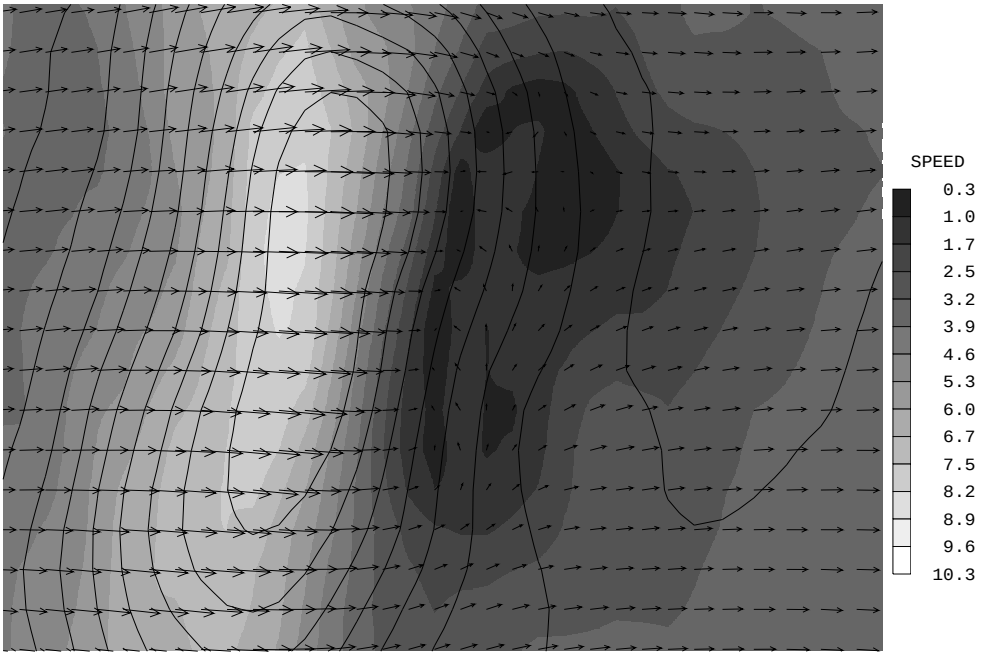

Figure 7: The velocity field with speed contours and velocity vectors at the lee side of Askervein Hill, 10 meters above the ground with standard $k - \varepsilon$ model

3.4 Torsnesaksla

Torsnesaksla is situated south of Tromsø in the northern part of Norway. The extension of the modelled area is 22×18 km, including the measuring masts at Hekkingen and Torsnesaksla, see figure 8.

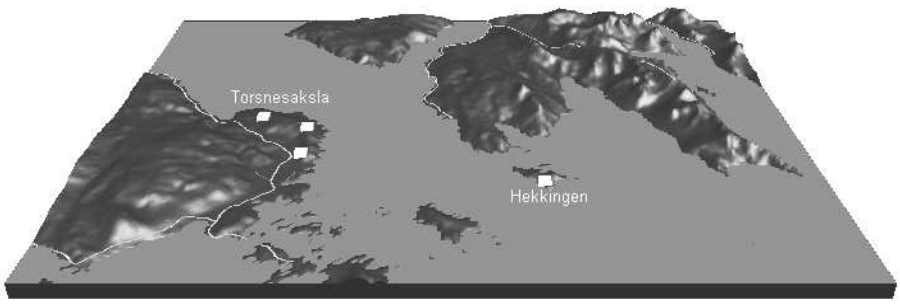

Figure 8: Torsnesaksla - meso scale model, view from north

3.4.1 Measurements

The meteorological station at Hekkingen lighthouse is used as a reference station with measurements at 10 meters height. At Torsnesaksla measurements have been undertaken since 01.05.98. The anemometers are situated at 20, 35 and 50 meters height. Two separate

time intervals of approximately 4 and 3 months have been analysed and compared against the reference station at Hekkingen. The Distance between Hekkingen and Torsnesaksla is about 8 km.

Normalised mean speeds with Hekkingen as reference station is given in table 3 for 12 sectors, (1=N, 4=E, 7=S, 10=W). Note that measurements at different heights are used in the tables. The cross correlations are low for several of the sectors. Table 4 shows the spreading in directional distribution.

Results from the 3 months interval were taken during the autumn when the average wind speeds are higher than in the 4 months interval. These results also give the highest cross correlations, and is probably the best suited for comparison with meso scale simulations. In general the low cross correlations indicate that micro scale effects are important at the measuring sites.

Sector	4 months interval		3 months interval	
	Normalised speed	Cross correlation	Normalised speed	Cross correlation
1	1.53	0.83	1.15	0.59
2	0.85	0.57	0.99	0.46
3	0.89	0.46	1.00	0.66
4	1.18	0.39	0.96	0.92
5	1.24	0.58	1.01	0.80
6	1.15	0.65	1.12	0.83
7	1.77	0.41	1.32	0.73
8	2.06	0.52	1.07	0.64
9	0.97	0.59	0.59	0.40
10	0.68	0.45	0.79	0.44
11	1.01	0.56	0.78	0.63
12	1.60	0.81	0.98	0.77

Table 3: Normalised speed, $\text{Torsnesaksla}_{50}/\text{Hekkingen}_{10}$, and cross correlations versus directions

3.4.2 Meso scale simulations

The meso scale model covers the area of 22×18 km given in figure 8. The model extension in vertical direction is 3000 meters above the heighest mountain.

The topography and roughness have been extracted from a digital terrain model (DTM) covering the total area of Norway. The resolution of the DTM is 100×100 m. However, due to limited computer resources, a rather coarse grid has been used in the simulations with cells of 400×400 m in the horizontal direction. With this grid resolution it will not be possible to capture micro scale effects.

In the vertical direction 20 cells have been used with a refinement towards the ground, situating the first grid point at approximately 25 meters height. Therefore, an attempt to compare the simulations with measurements at 10 meters height must be based on extrapolation. In the results presented in figure 9, the measurements from the two time intervals presented in the above section are compared against results from the simulations at 50 meters height. The simulation results have also been adjusted with a factor equal to 1.2, which is the ratio between the speed at 50 meter and 10 meter using a logarithmic

Torsnesaksla → Hekkingen		1	2	3	4	5	6	7	8	9	10	11	12
	1	58	3	0	0	8	4	4	4	1	1	10	53
	2	124	14	3	5	5	9	5	7	1	9	8	51
	3	35	8	15	3	16	16	6	0	1	3	3	20
	4	12	6	13	7	13	21	2	2	0	1	3	10
	5	7	4	14	8	54	51	20	4	2	2	4	14
4 months	6	6	0	5	29	634	274	93	2	0	3	7	3
	7	4	4	1	14	34	17	31	5	0	1	2	3
	8	4	0	1	1	13	11	27	10	4	1	0	1
	9	7	2	0	4	18	17	38	15	11	10	3	5
	10	26	5	2	1	16	22	31	18	26	61	35	18
	11	105	3	3	4	23	23	15	11	2	18	53	97
	12	85	2	3	2	9	13	15	6	1	6	30	115
	1	115	1	1	1	5	9	9	2	3	1	9	110
	2	41	10	9	2	5	7	6	0	2	1	1	15
	3	1	0	17	2	0	4	2	0	0	1	0	1
	4	2	1	5	4	2	2	0	0	0	0	0	0
	5	3	1	11	2	5	0	2	0	0	0	0	0
3 months	6	6	4	8	15	685	143	15	1	2	1	1	5
	7	1	1	4	20	253	73	38	2	1	0	1	6
	8	6	3	1	1	3	19	26	14	9	4	4	5
	9	3	1	0	0	2	5	12	2	11	3	2	1
	10	2	0	0	0	1	3	4	4	2	3	0	6
	11	6	0	0	1	1	2	2	1	0	0	9	13
	12	29	1	0	1	6	10	4	1	4	0	53	77

Table 4: Directional distribution of measurements samples, 4 and 3 months measuring intervals

profile with roughness height set to 0.01. The logarithmic profile is only valid over flat terrain, which clearly is violated at the measuring sites. Most likely the adjustment factor will be less than 1.0 for sectors with speed–ups effects. This serves as an illustration of the difficulties encountered when comparing results affected by micro scale effects with a meso scale model. Although a comparison should be treated with care, it is still possible to detect similar trends in the simulations and the measurements. Southern wind, which is the dominating wind direction, shows the highest speed–up in agreement with the measurements.

The actual measuring site at Torsnesaksla is situated in the corner of a 400×400 m cell, as the averaged wind speed is calculated in the cell center, the adjacent cells could equally well be compared against the measurements. As a measure of this sensitivity, results from adjacent cells have also been presented in figure 9. Finally, a vector plot of the dominating wind direction is given, in figure 10.

Both the standard and modified $k - \varepsilon$ model have been tested. The discrepancies in the calculated normalised speeds are marginal, the displayed results are those with the standard $k - \varepsilon$ model. Profiles for k and ε developed in sub–models and the analytical profiles described in section 2.2 have also been tested. Again there was no noticeable effect on the normalised speeds.

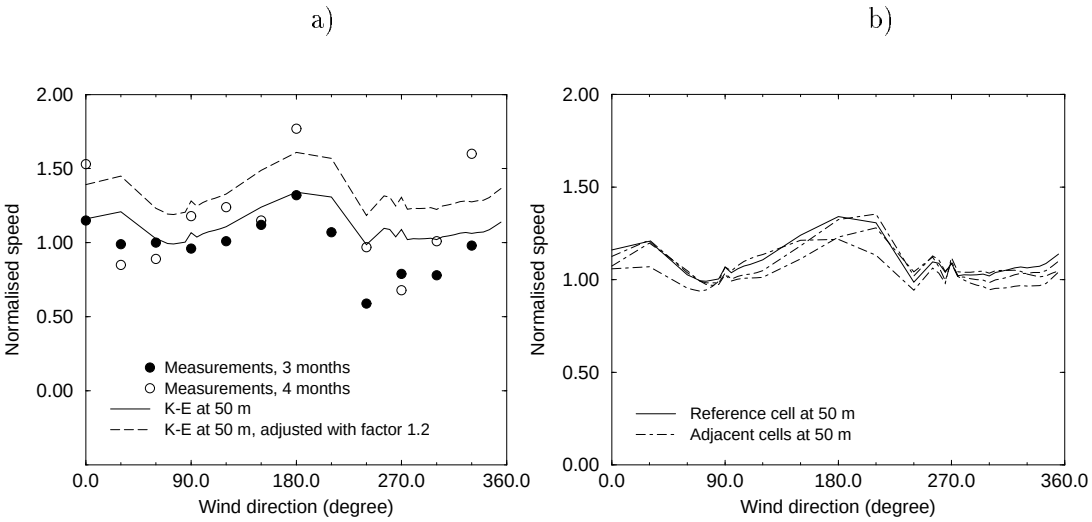

Figure 9: Normalised speed
a) Torsnesaksla/Hekkingen reference cell versus measurements
b) Torsnesaksla/Hekkingen adjacent cells

Figure 10: Velocity fields for wind direction 150°, height contour interval is 100 meter

3.4.3 Micro scale simulations

At both measuring sites, scale effects below the meso scale grid resolution is important. In figure 11 the topography at Torsnesaksla is presented with a resolution of 5×5 meter, the height elevation along a line in east-west direction is also given in the figure. In the meso scale model this line section was resolved with 10 cells. In a refined model the grid size is reduced to 100×100 meter. Obviously, the velocity field at the grid points adjacent to the ground displays a more detailed pattern in this refined model. Figure 12 gives an example with wind direction from 210°. A 100×100 meter cell marks the position of the measuring site, included is also the adjacent 400×400 meter cells in the meso scale model. Note that there has been no interpolation of boundary conditions between the two models, comparison of results in the vicinity of the borders will not be possible.

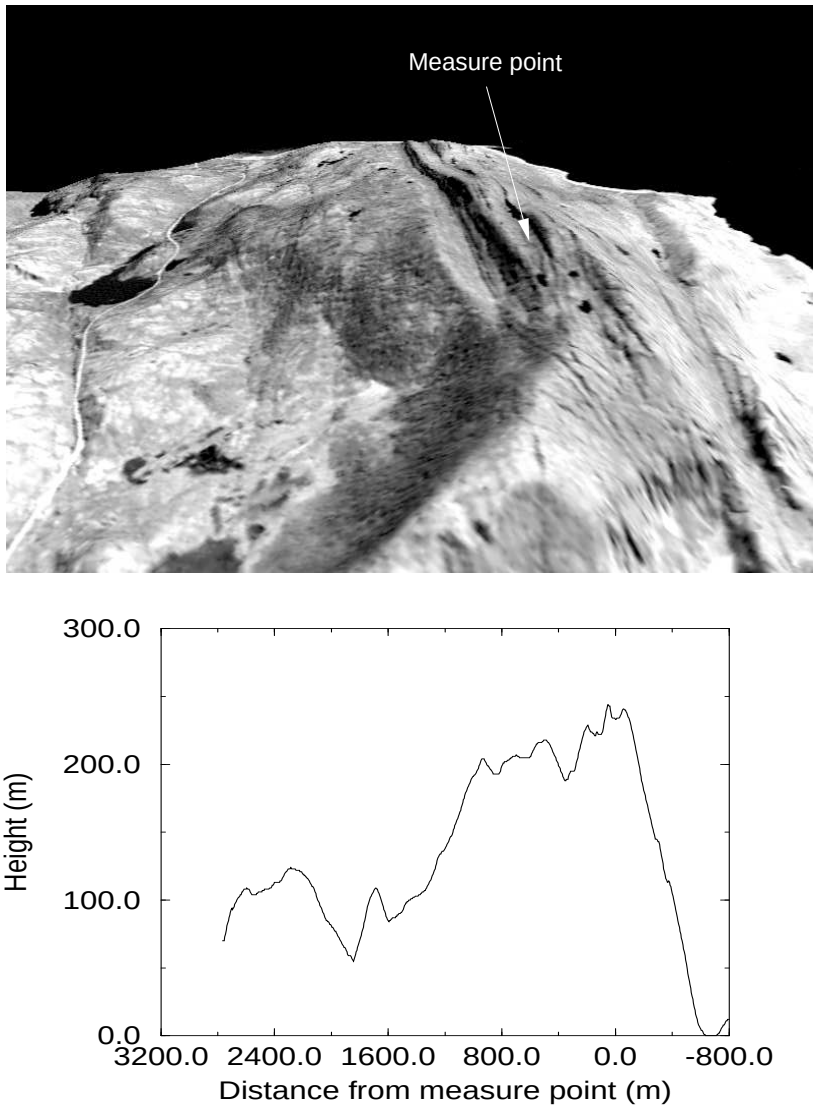

Figure 11: Topography at Torsnesaksla with grid resolution 5×5 meter, view from north (upper), height in east-west direction through measure point (lower)

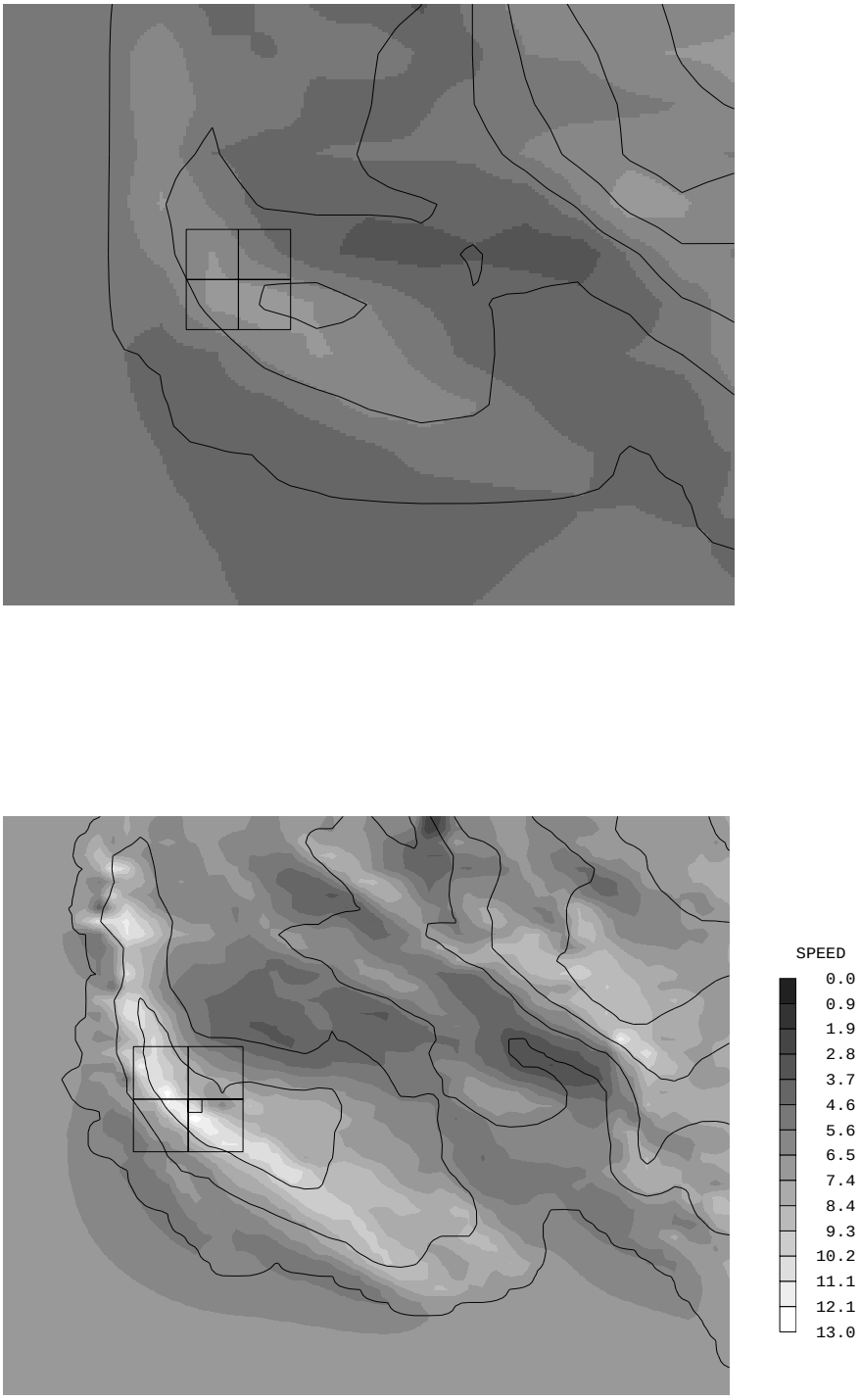

Figure 12: Speed contours for coarse (upper) and fine (lower) model, wind direction 210°, height contour interval is 100 meter.

4 Further work

The measurement data will be more representative as longer time series become available at Torsnesaksla. The meso scale simulations will be recalculated on a finer grid. Finally the development of an interface between meso and micro models will facilitate model nesting.

5 Summary and conclusions

A verification of the Reynolds averaged Navier–Stokes solver WIND–SIM has been performed. The verification started on simplified terrain and moved on towards complex terrain. It was of particular interest to gain insight into the errors made in meso scale modelling of complex terrain with grids to coarse to reflect the underlying topography.

A site in the northern part of Norway, with complex geometry and two measuring masts 8 km apart, was chosen. Although both measuring sites are affected by micro scale effects, similar trends are observed in the the simulations and the measurements. However, the case also illustrates the difficulties encountered when comparing simulations and measurements obtained on different length scales. The discrepancies is due to:

- Measurement series to short to represent mean velocities
- Meso scale model which does not resolve micro scale effects
- Incomplete physical model

Acknowledgements

This study was supported by The Research Council of Norway, under NYTEK project 126645/212. The author would also like to thank Norsk Miljøkraft for making the measurement data at Torsnesaksla available to the project, likewise the Institutt for Energiteknikk for their preparation of the measurements.

References

[Alm and Nygaard (1995)] Alm, L. K. and Nygaard, T. A. (1995), "Flow over complex terrain estimated by a general purpose Navier–Stokes solver", *Modeling, Identification and Control*, 16(3), 169–176.

[Baklanov et al. (1997)] Baklanov, A., Burman, J., and Näslund, E. (1997), "Numerical modelling of three–dimensional flow and pollution transport over complex terrain", *The Phoenics Journal*, pages 57–86.

[Detering and Etling (1985)] Detering, H. W. and Etling, D. (1985), "Application of the E - ε turbulence model to the atmospheric boundary layer", *Boundary–Layer Meteorology*, 33, 113–133.

[Grundberg (1994)] Grundberg, S. (1994), "Simulation of the surface layer of a stratified atmosphere using PHOENICS", *The Phoenics Journal*, 7(1), 8–33.

[Huser et al. (1997)] Huser, A., Nilsen, P. J., and Skåtun, H. (1997), "Application of $k-\varepsilon$ model to the stable ABL: Pollution on complex terrain", *Journal of Wind Engineering and Industrial Aerodynamics*, 67&68, 425–436.

[Lemelin et al. (1988)] Lemelin, D. R., Surry, D., and Davenport, A. G. (1988), "Simple approximations for wind speed-ups over hills", *Journal of Wind Engineering and Industrial Aerodynamics*, 28, 117–127.

[Näslund et al. (1992)] Näslund, E., Svensson, U., and Karlsson, E. (1992), "Boundary–layer flow over Sundsvall", *The Phoenics Journal*, pages 222–238.

[Panofsky et al. (1977)] Panofsky, H. A., Tennekes, H., Lenschow, D. H., and Wyngaard, J. C. (1977), "The Characteristics of Turbulent Velocity Components in the Surface Layer Under Convective Conditions", *Boundary–Layer Meteorology*, 11, 355–361.

[Taylor and Teunissen (1987)] Taylor, P. A. and Teunissen, H. W. (1987), "The Askervein Hill Project: overview and background data", *Boundary–Layer Meteorology*, 39, 15–39.